AJR FOCUS ON:

Low-Flow Vascular Malformation Pitfalls: From Clinical Examination to Practical Imaging Evaluation—Part 1, Lymphatic Malformation Mimickers

Candace L. White[1]
Brandon Olivieri[1]
Ricardo Restrepo[2]
Brett McKeon[2]
S. Pinar Karakas[3]
Edward Y. Lee[4]

OBJECTIVE. Palpable subcutaneous masses present in various shapes and sizes in the pediatric population and, accordingly, represent a variety of underlying causes. Lymphatic and venous malformations are among the most common pediatric subcutaneous lesions. However, there are congenital and acquired, as well as benign and malignant, soft-tissue masses that can mimic them clinically and at imaging.

CONCLUSION. Here, we review the natural history, wide range of clinical presentations, and varied but characteristic imaging appearance of lymphatic malformations that can pose diagnostic difficulties in children. In addition, the clinical and imaging characteristics of some pediatric soft-tissue pathologies that can mimic lymphatic malformations and clues to reach a proper diagnosis are highlighted.

Keywords: lymphatic, lymphatic malformation, mimic, pitfall, slow-flow malformation, vascular malformation

DOI:10.2214/AJR.15.15793

Received October 17, 2015; accepted after revision December 15, 2015.

Based on a presentation at the ARRS 2014 Annual Meeting, San Diego, CA.

[1]Department of Radiology, Mount Sinai Medical Center of Florida, Miami Beach, FL.

[2]Department of Radiology, Nicklaus Children's Hospital, Miami Children's Health System, 3100 SW 62nd Ave, Miami, FL 33155. Address correspondence to R. Restrepo (Ricardo.Restrepo@MCH.com).

[3]Department of Radiology, Benioff Children's Hospital at Oakland, University of California at San Francisco, Oakland, CA.

[4]Department of Radiology, Boston Children's Hospital. Boston, MA.

WEB
This is a web exclusive article.

AJR 2016; 206:W1–W12

0361–803X/16/2065–W1

Vascular malformations are not neoplasms but rather congenital endothelial malformations that result from errors in vascular morphogenesis [1, 2]. Though a complete discussion of vascular malformation classification is beyond the scope of this review, vascular malformations can be mainly delineated histologically into lymphatic, capillary, venous, arteriovenous, or mixed malformations (any combination) [3–6]. Vascular malformations can also be classified as low-flow and high-flow according to their hemodynamic characteristics [1, 3]. The low-flow vascular malformations are composed of nonarterial components and include capillary, venous, and lymphatic malformations [3, 4]. Because low-flow vascular malformations lack arteriovenous shunting, increased temperature and pulsatility are absent on physical examination. The diagnosis of capillary malformations, which consist of port wine stains and telangiectasia, is made clinically, with imaging playing virtually no role. Most capillary malformations are isolated anomalies; however, they can be part of a syndrome or can herald an associated deeper vascular malformation for which imaging evaluation is required. Venous malformations have a variable clinical presentation according to their depth and extent as well as the presence of thrombosis. Likewise, on imaging, venous malformations have different morphologic patterns, posing a significant source of diagnostic overlap with benign and malignant neoplasms. The high-flow types are composed of arterial components, including arteriovenous malformation and arteriovenous fistulas [3–5]. Low-flow vascular malformations, specifically lymphatic and venous malformations, are among the most common soft-tissue masses seen in a pediatric practice; the reported frequencies are estimated to be 1 in 12,000 births for macrocystic lymphatic malformation and 1 in 10,000 births for venous malformations [7–9].

Lymphatic malformations are diagnosed by the clinician according to history and physical examination; imaging is usually required for confirmation of the diagnosis, to evaluate the lesion's extent, or for therapeutic planning. Lymphatic malformations may have an atypical and delayed presentation, not only clinically but also on imaging. Likewise, certain soft-tissue masses in children can mimic lymphatic malformations in many ways. To decrease the risk of misdiagnosis, radiologists, especially interventional radiologists, should adopt an active role when dealing with lymphatic malformations and other vascular anomalies in children. On the one hand, a thorough clinical history should be obtained, and the child should be examined carefully at the time of imaging or during a previous formal consultation. If any intervention is requested, it is preferably performed

in an institution with a dedicated vascular malformation clinic and by experienced radiologists. On the other hand, radiologists should be familiar with the imaging spectrum of these lesions and with some common mimickers in the pediatric population so that prompt and accurate diagnosis can be achieved and optimal patient care provided.

The overarching goal of this article is to provide an up-to-date review of a variety of pediatric soft-tissue pathologies that can mimic lymphatic malformations and clues to minimize the risk of misdiagnosis and delayed treatment. The natural history, clinical presentation, and varied but characteristic appearance on different imaging modalities of lymphatic malformations are highlighted.

Clinical Appearance of Lymphatic Malformations

Lymphatic malformations are low-flow vascular malformations consisting of dilated lymphatic vessels without cellular atypia, forming cystlike structures separated by fibrous septa. The mechanism of origin results from aberrant lymphatic morphogenesis related to a failure of communication with the venous system, rendering lymphatic malformations isolated from the otherwise normal lymphatic system [2, 4, 10–12]. Lymphatic malformations occur after the arrest of lymphatic system development at early stages of embryogenesis, thereby resulting in multilocular, rather than the rare unilocular, lesions [13–16]. Three subtypes based on morphologic features have been described: macrocystic, microcystic, and combined [17]. The macrocystic subtype is composed of locules measuring greater than 1 cm, the microcystic subtype comprises smaller (usually subcentimeter) cysts, and the combined subtype shares features of both (Fig. 1).

Lymphatic malformations most commonly involve the subcutaneous tissues, with a reported 70–80% occurrence in the head and neck, but they can occur throughout the body [3, 18]. Lymphatic malformations are well known to be transspatial, disregarding anatomic and fascial boundaries, and they can involve multiple tissue planes. In some cases, lymphatic malformations cause mass effect on adjacent structures, which can lead to soft-tissue and osseous hypertrophy and potential limb-length discrepancy [10–12, 19, 20].

Like all vascular malformations, lymphatic malformations are congenital and grow proportionally to the systemic growth of the patient. They are usually identified during early childhood, with 50–65% identified at birth, 80–90% found by age 2 years, and rare de novo identification occurring beyond adolescence [7, 21]. Clinically, undisturbed lymphatic malformations are characteristically described as painless soft supple lesions that are not necessarily compressible [22–24]. Lymphatic malformations transilluminate, have an intact overlying skin, and lack temperature changes in their natural state. Furthermore, no pulsatility or bruit is palpated

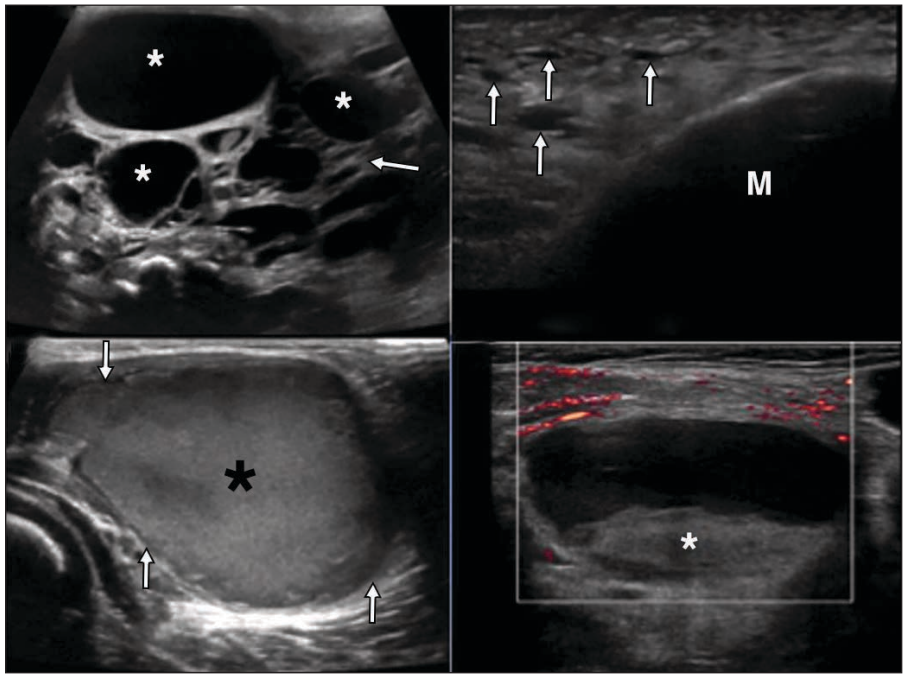

A

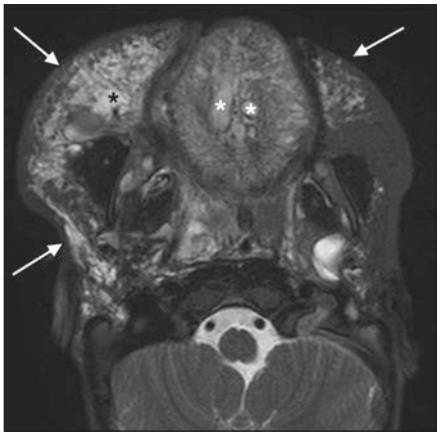

B

Fig. 1—Various imaging appearances of lymphatic malformations in six different patients.
A, Lymphatic malformations in three patients. In top left image, mixed undisturbed cervicofacial lymphatic malformation is seen in 12-day-old boy. Lymphatic malformation has macrocysts (*asterisks*) and microcysts (*arrow*) containing anechoic fluid separated by fibrous septa. In top right image, typical appearance of microcystic lymphatic malformation is seen in 2-year-old boy. High-resolution gray-scale ultrasound (US) image of face shows thickening of subcutaneous fat and loss of normal fascial planes due to microcystic lymphatic malformation with several tiny microcysts (*arrows*). M = malar bone. In bottom images, lymphatic malformation containing blood at different stages is seen in 3-month-old boy. High-resolution US image of axillary locule (*bottom left*) shows macrocyst (*arrows*) containing low-level echoes (*asterisk*) due to hemorrhage, and high-resolution US image of another locule (*bottom right*) shows soft-tissue nodule (*asterisk*) in dependent portion of macrocyst with no color flow, consistent with retracted mural thrombus.
B, 2-year-old boy with microcystic lymphatic malformation. Axial T2-weighted MR image shows extent of microcystic lymphatic malformation seen as poorly defined hyperintense areas in subcutaneous soft tissues of right hemiface and left cheek anteriorly (*arrows*) with involvement of tongue and right parotid gland. Few microcysts are discernible (*asterisks*).

(Figure 1 continues on next page)

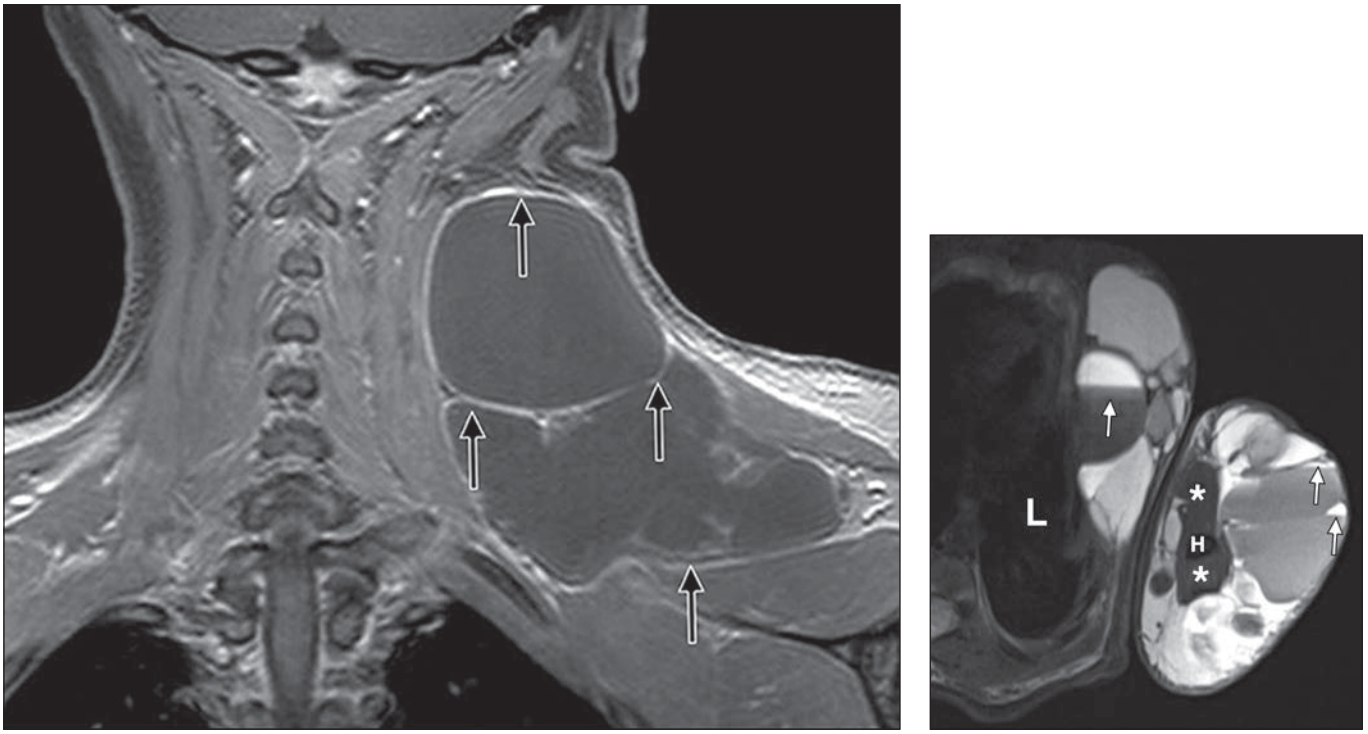

Fig. 1 (continued)—Various imaging appearances of lymphatic malformations in six different patients.
C, 9-year-old girl with undisturbed macrocystic lymphatic malformation of neck. Coronal contrast-enhanced T1-weighted MR image with fat saturation shows faint septal and capsular contrast enhancement (*arrows*). No enhancing solid component is seen.
D, 3-month-old boy with mixed (macro- and microcystic) lymphatic malformation containing blood at different stages involving left chest wall and arm. Axial T2-weighted MR image shows large extension of lymphatic malformation. Lesion contains locules of different sizes and various signal intensities, some of which contain fluid-fluid levels (*arrows*) indicative of blood at different stages. In arm, lymphatic malformation is causing mass effect on musculature (*asterisks*). L = lung, H = humerus.

TABLE 1: Suggested MRI Protocol for a Suspected Vascular Malformation

Sequence	What to Look For
Coronal (less frequently sagittal) STIR or T2-weighted sequence with fat saturation	Evaluates the extent of the lesion
Axial T1-weighted sequence	Evaluates the contents: blood, proteinaceous material, fat, and involvement of adjacent musculature
Axial STIR or T2-weighted sequence with fat saturation	Evaluates relationship with adjacent structures: skin, neurovascular bundle, and bone
Axial gradient-recalled echo T1-weighted sequence	Evaluates for the presence of phleboliths, recent bleed, or flow voids in hypervascular lesions
Axial T1-weighted sequence with fat saturation before gadolinium enhancement	Required to evaluate enhancement pattern
2D Time-of-flight MR angiogram and MR venogram[a]	To evaluate vascular supply, deep venous system, and flow characteristics
Multiple phase gadolinium-enhanced MR angiogram[a]	To evaluate flow dynamics
Axial T1-weighted sequence with fat saturation after gadolinium enhancement	Evaluates enhancement pattern: dynamics and possible solid component
Second plane T1-weighted sequence with fat saturation after gadolinium enhancement	Evaluates delayed enhancement: very useful in venous malformations

[a]Optional sequences if dealing with a lymphatic malformation with certainty or in the follow-up of venous malformations.

on clinical examination [19–23]. The clinical appearance of lymphatic malformations may vary, because they tend to respond to different stimuli, which is a potential source of confusion. Lymphatic malformations are predisposed to sudden growth as a response to immunologic stimuli (most frequently, a common cold), hemorrhage, or infection of the lesion itself. Because of the pliability of the walls, lymphatic malformations can experience tremendous sudden changes in size, which, in turn, can lead to hemorrhage and further growth due to stretching of the capsular or septal vessels. The lymphatic malformations then become painful and firm, with a bluish or purplish hue, simulating a venous malformation or a hematoma (Fig. 2). Lymphatic malformations are also predisposed to infection by bacterial seeding [25, 26]. When infected, lymphatic malformations often become larger, painful, indurated, and erythematous [20, 27, 28] (Fig. 2). Likewise, disturbed lymphatic malformations frequently have a tendency to return to

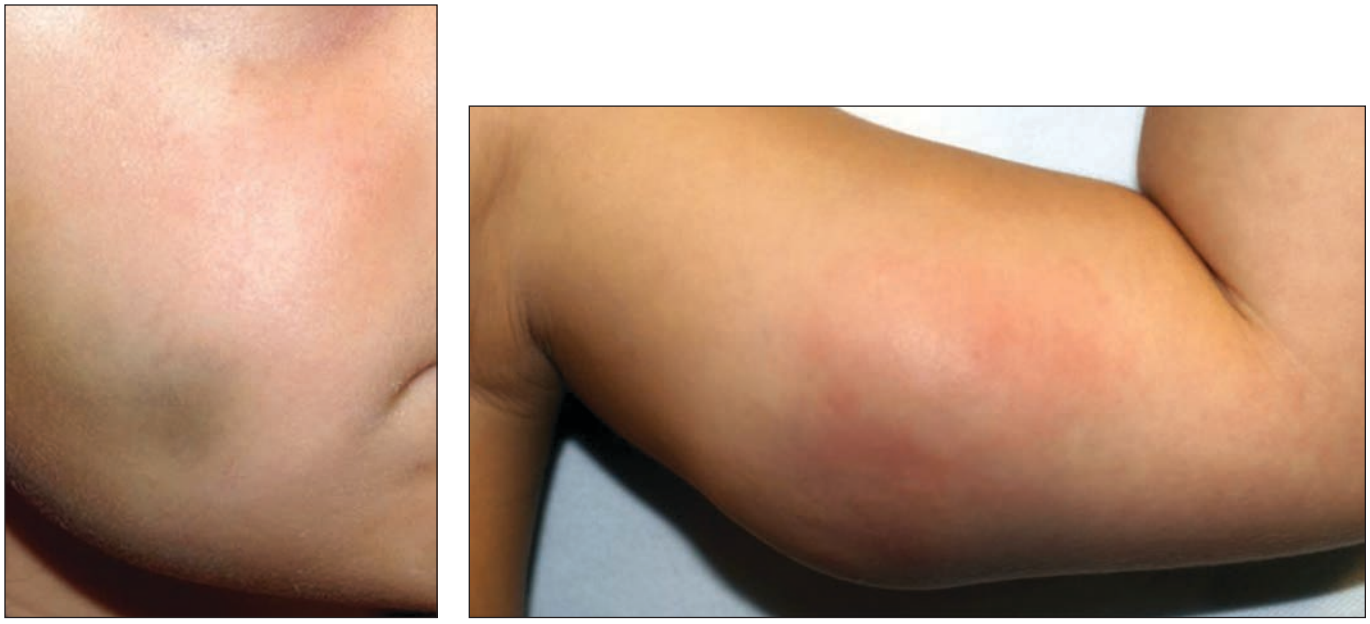

Fig. 2—Two patients with lymphatic malformations.
A, 4-year-old girl with right cheek lymphatic malformation with bleed who presented with bruising after playing in park. Localized mass in right cheek with purplish discoloration is seen. Mass was tender and firm on palpation with no increased temperature.
B, 3-year-old boy with infected lymphatic malformation who presented with sudden development of painful mass on left arm with overlying skin erythema and induration.

baseline size after the stimulus has subsided. However, complete resolution of the lesion rarely occurs without intervention.

Imaging Appearance of Lymphatic Malformations

Ultrasound (US) is usually the first-line imaging modality in the diagnostic workup of lymphatic malformations, especially when they are small and superficial, in the pediatric population. Contrast-enhanced MRI is the preferred complementary imaging modality to US in evaluation of lymphatic malformations. MRI is of particular value for deeply seated and extensive lesions, evaluation of lesion size and extent of tissue involvement, and preprocedural planning (Table 1). CT with IV contrast material is a less preferred alternative to MRI because of the decreased contrast resolution and the use of ionizing radiation, but it is an acceptable alternative should MRI not be available.

The classic sonographic appearance of lymphatic malformations is that of multiloculated cystic masses with imperceptible walls, which are anechoic in the natural state, offering posterior acoustic enhancement (Fig. 1). Lymphatic malformations are rarely unilocular; in fact, a unilocular cystic mass is unlikely to be a lymphatic malformation. Internal floating low-level echoes or fluid-fluid levels—representing blood, pus, or chyle—may be present [11, 18, 19, 29]. In cases of acute hemorrhage, the affected locules display increased echogenicity and contain floating low-level echoes. With time, fluid-fluid levels and, eventually, a retracted clot may form (Fig. 1). Intralesional retracted clots are seen as solid areas of different echogenicities with no internal vascularity on color Doppler US (or contrast enhancement on CT or MRI). Regardless of the state (natural or inflamed), pure lymphatic malformations have no associated soft-tissue component, and no internal flow is present on color Doppler examination. However, minute arteries and veins may be visible within the fibrous septations and capsule [11, 18, 19, 29]. No perilesional inflammation should be present unless there is active infection. In cases of infection, debris or echogenic fluid is seen, and hyperemia along the capsule and septa develops.

The role of color Doppler US to differentiate benign from malignant masses has been evaluated with limited success. Some studies in adults have shown that an organized vascular pattern, although not pathognomonic, is more commonly seen in benign soft-tissue masses, whereas a chaotic vascular pattern with randomly distributed tortuous vessels displaying abrupt variation in caliber is more commonly seen with malignancies [30–32]. In the case of lymphatic malformations, because they are multiseptate masses, minimal, if any, peripheral and septal vascularity that can be accentuated during periods of hemorrhage or infection is expected. When considering the mean end diastolic volume and mean resistive index, significant overlap between benign and malignant lesions has been found; therefore, the role of Doppler US to exclude malignancy is of limited clinical value [30, 33]. In our experience, color Doppler US of soft-tissue masses, including lymphatic malformations that are usually diagnosed during the first few years of life, is further compromised by the lack of cooperation in children.

On MRI, lymphatic malformations are seen as multiloculated cystic masses with fluid signal and no flow voids [23] (Fig. 1). In cases of hemorrhage or infection, the intralesional signal changes according to the acuity of the process, and fluid-fluid levels may develop (Fig. 1). Faint septal and capsular enhancement may be naturally present, which can be more vivid in the setting of inflammation, but no enhancing solid component should be present [11] (Fig. 1). T2-weighted MRI with fat saturation or STIR sequences can highlight the presence of perilesional inflammation seen only in cases of active inflammation. Microcystic lymphatic malformations occasionally can appear as solid

masses with scant tiny cysts, or no perceptible cysts at all, causing thickening and obliteration of the tissue planes.

In addition to their variable appearance on imaging, not only morphologically (e.g., macrocystic, microcystic, or mixed) but in terms of their contents (e.g., natural state, stimulated, infected, or hemorrhagic), lymphatic malformations can pose diagnostic difficulties, particularly in the pediatric population, for four main reasons. First, lymphatic malformations are congenital and always present at birth, but they are not always apparent clinically or at imaging, causing inherent confusion when they are noticed later in childhood. Second, some soft-tissue malignancies affecting children are low grade, growing very slowly in a fashion similar to lymphatic malformations [34]. Third, pediatric malignancies can be well circumscribed; when they are necrotic, they can be predominantly cystic and can bleed, producing fluid-fluid levels, and they may not show internal vascularity at imaging, features that are fairly typical of lymphatic malformations [30, 33–38]. Similarly, aggressive neoplasms may contain fluid-fluid levels because of their rapid growth. Fourth, several nonneoplastic congenital cysts in children occur in locations that overlap with those of lymphatic malformations (e.g., head, neck, and superficial subcutaneous soft tissues). These cysts are slow growing and can become infected later in life.

Neoplasms in Neonates and Infants That Can Mimic Lymphatic Malformations

Perinatal neoplasms (congenital and neonatal, when defined as those seen at birth and in the first 60 days of life, respectively) represent less than 3% of all pediatric neoplasms, with the frequency of malignancy ranging from 0.003% to 1.9% [39, 40]. Perinatal neoplasms may pose a diagnostic dilemma because of a lack of awareness and the rarity of these tumors (about 1/10,000 live births, with a reported variation of 12–121 per million live births) [40–43]. Neoplasms in the perinatal period can also mimic the much more common vascular malformations clinically and at imaging. In a study by McCarville et al. [44] of 30 infants with soft-tissue malignancies, the most common diagnoses were rhabdomyosarcoma (RMS), congenital fibrosarcoma, and other non-RMS neoplasms.

Teratoma

Teratomas are true germ cell neoplasms composed of tissue derived from more than one embryologic layer (ectoderm, endoderm, and mesoderm) that are usually foreign to the anatomic site of origin. Teratomas originate anywhere along the midline, with extragonadal locations occurring primarily in neonates. Teratomas are the most common congenital perinatal tumors, accounting for up to 36% of all cases; the most common locations are the sacrococcygeal and cervicofacial regions [45–47]. Cervicofacial teratomas account for nearly 2% of all neonatal tumors, with a reported frequency between 1 in 40,000 and 1 in 80,000 live births [42, 45, 47, 48]. Teratomas in the cervicofacial region share similar features with lymphatic malformations. Besides the location, cervicofacial teratomas can be seen prenatally, can be associated with polyhydramnios, and frequently are large and bulky with secondary mass effect on the airway and adjacent structures. It can be difficult to distinguish these neoplasms from lymphatic malformations by imaging because they often are multiloculated predominantly cystic masses (Fig. 3). The presence of fat and calcifications, whether dystrophic or in the form of mineralized bone, is critical for the diagnosis of a teratoma (Fig. 3). However, some teratomas do not have macroscopic fat or calcium at imaging [49, 50]. CT may play an important role in the diagnosis because fat and especially calcifications are readily identified by this modality. As for any other neoplasm, the presence of soft tissue is also a supporting finding in the diagnosis of teratomas [51]. A feature that we find useful in differentiating teratomas from lymphatic malformations is the associated skeletal changes with the former, causing bone remodeling, scalloping, and splaying (Fig. 3). Skull-base invasion with widening of the neural foramina is also possible. In contrast, lymphatic malformations, being low-flow lesions of a low-

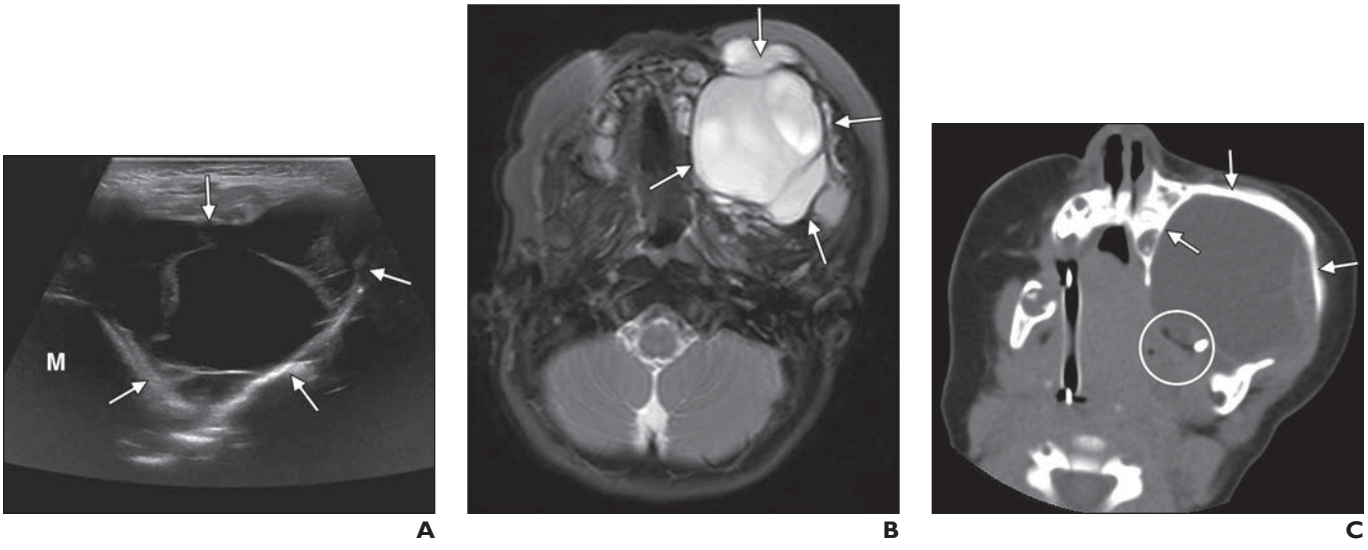

Fig. 3—1-year-old girl with diagnosis of teratoma presenting with progressive painless facial swelling since birth.
A, Ultrasound image of face shows large multiseptate cystic mass (*arrows*) in left cheek. M = malar bone.
B, Axial T2-weighted MR image with fat saturation of face shows septate hyperintense left cheek mass (*arrows*) suggesting cystic nature.
C, Axial CT image without contrast agent shows left cheek mass as hypodense due to cystic component. Peripheral nodule containing fat and coarse calcification (*circle*) is readily visible and highly suggestive of teratoma. Note bone remodeling involving left maxilla and zygomatic arch (*arrows*).

pressure system, do not cause these skeletal changes. Later in life, bone expansion and hypertrophy may occur [52–54]. The prenatal sonographic detection of the lesion may provide an important diagnostic clue because lymphatic malformations can be detected as early as the first trimester. Teratomas, however, are detected in the second trimester [55]. A deeply seated mass in the nasopharynx with cystic components in the presence of bone remodeling is more likely to be a teratoma than a lymphatic malformation in the first year of life, especially if calcifications and fat are present [52].

Rhabdomyosarcoma

At this age, RMS can present as large masses occurring nearly anywhere in the body, with a substantial number in the head and neck, similar to lymphatic malformations. This neoplasm may have clinical and imaging appearances similar to those of vascular malformations that usually present as a painless mass in the pediatric population. On palpation, RMS are firmer than lymphatic malformations (in the absence of a cystic component) and have a tendency toward rapid growth, which is different than undisturbed lymphatic malformations. However, when hemorrhagic, lymphatic malformations harden and grow suddenly in a pattern similar to that of congenital RMS. RMS is one of the most common childhood sarcomas, with reports of misdiagnosis as a vascular malformation [56]. Lesions presenting as a solitary fully formed mass at birth or as a rapidly growing tumor, particularly on the face and neck, are more likely to be misdiagnosed as vascular anomalies. On imaging, RMS can have large cystic components and fluid-fluid levels due to hemorrhage and necrosis, in a fashion similar to that of lymphatic malformations, especially with rapid growth (Fig. 4). However, the presence of solid components with color flow on US or contrast enhancement on MRI or CT supports the diagnosis of RMS (Fig. 4). Not infrequently, congenital RMS has widespread metastatic disease at presentation because of its aggressive behavior, which is another supportive diagnostic clue [44, 57] (Fig. 4). Ultimately, if a congenital RMS cannot be definitively distinguished from a lymphatic malformation by imaging, a biopsy may be warranted for a definitive diagnosis.

Lipoblastoma

Another potential diagnostic pitfall in infancy is lipoblastoma. Lipoblastomas are rare mesenchymal tumors of embryonal white fat. They commonly present in infancy and early childhood, with 99% of cases presenting before age 3 years [58]. In most cases, lipoblastomas are easily clinically distinguishable from lymphatic malformations because they are rubbery and firmer masses, and on imaging, the presence of fatty elements is virtually diagnostic at this age. A subset of lipoblastomas can be confused with lymphatic malformations because of the presence of a large myxoid component. Clinically, these lesions and lymphatic malformations can share the same presentation, which includes soft painless enlarging masses with variable growth rates that commonly occur in the lower extremities or cervical region and have intact overlying skin. These two entities also share a similar age range. Transillumination with a flashlight is usually not present in lipoblastomas.

The imaging appearance of lipoblastomas is variable depending on the tissue composition, usually with mixed fatty and myxoid stromal components, and with younger patients having a greater myxoid component [58–61]. The imaging appearance of myxoid lipoblastomas and lymphatic malformations can be strikingly similar. The myxoid component of lipoblastomas is hypoechoic on US and has low attenuation on CT. On MRI, the myxoid component shows a low T1 signal and a high signal on T2-weighted MR images with fat saturation similar to that of lymphatic malformations (Fig. 5). After gadolinium administration, variable contrast enhancement can be peripheral and septal, which is also identical to that of lymphatic malformations. Furthermore, lipoblastomas may have cystic spaces filled with mucoid material and vascular fibrous septa [62–64]. When there are fatty elements on T1-weighted MR images, the diagnosis of lipoblastoma is almost certain [59–61].

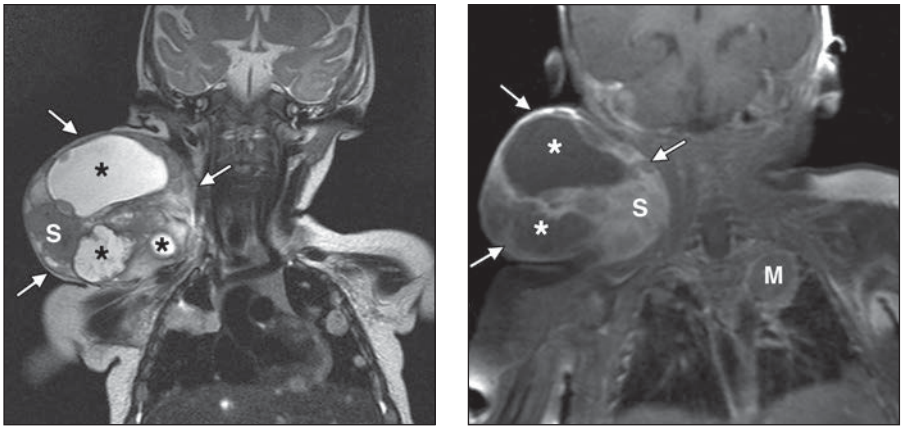

Fig. 4—3-week-old boy born with congenital rhabdomyosarcoma presenting as rapidly growing hard mass in right side of neck.
A, Coronal T2-weighted MR image shows interspersed cystic (*asterisks*) and solid areas (S) within mass (*arrows*). Multiple pulmonary and hepatic hyperintense nodules are seen, indicative of metastases.
B, Coronal contrast-enhanced T1-weighted MR image shows enhancement of solid areas (S) and lack of enhancement in cystic areas (*asterisks*) of mass (*arrows*). M = pulmonary metastasis.

Neoplasms in the Older Child That Can Mimic Lymphatic Malformations

Occasionally, malignant soft-tissue neoplasms that typically present in the older child and adolescent can be confused with lymphatic malformations because of their slow growth and cystic nature. The lack of differentiating imaging features confounds the diagnosis because the superficial nature of subcutaneous lesions often allows identification of lesions at a small size, and because vascularity correlates with tumor size, malignant lesions may appear hypovascular or avascular [31, 33]. This is complicated when these neoplasms share the common locations of lymphatic malformations (e.g., head, neck, and extremities) in the pediatric population.

Synovial Sarcoma

Synovial sarcoma (SS) is the second most common pediatric soft-tissue sarcoma, with approximately 30% of cases occurring in children and adolescents [65]. Between 70% and 95% of SS cases occur in the extremities, typically in a juxtaarticular location, but they can arise anywhere in the body [66, 67]. Clinically, SSs are slow-growing lesions

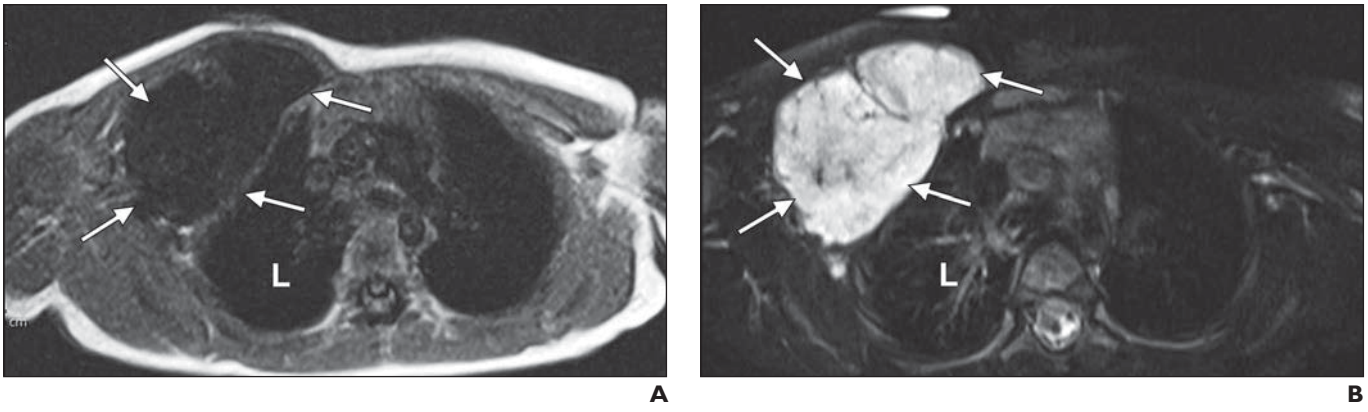

Fig. 5—3-month-old boy with chest wall lipoblastoma presenting as supple painless lump.
A, Axial T1-weighted MR image with no fat saturation shows well-defined hypointense oval mass (*arrows*) in deep tissues of right side of chest wall. L = lung.
B, Axial T2-weighted MR image with fat saturation shows mass (*arrows*) becoming homogeneously hyperintense, simulating cystic lesion. Several internal septations are now conspicuous. L = lung.

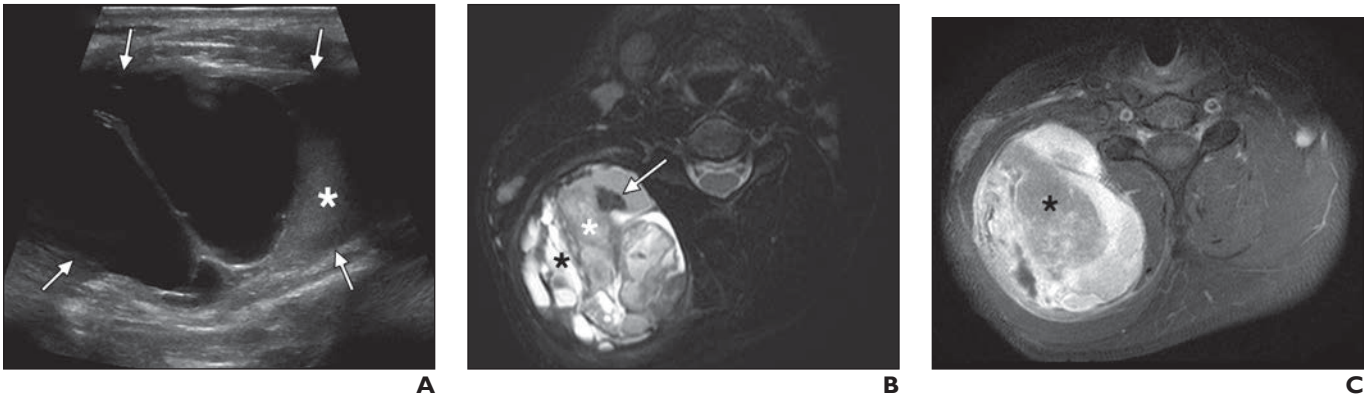

Fig. 6—11-year-old boy with synovial sarcoma presenting as slow-growing painless lump in posterior neck. Lesion was initially diagnosed as lymphatic malformation.
A, Ultrasound image shows mainly cystic mass (*arrows*) with thick septations and echogenic area (*asterisk*) that was interpreted as debris. No color Doppler ultrasound was used.
B, Axial T2-weighted MR image with fat saturation shows mainly cystic multiseptate mass in right and posterior neck containing areas of different signal intensities (triple sign): hypointense (*arrow*), intermediate (*white asterisk*), and hyperintense (*black asterisk*) signals.
C, Axial contrast-enhanced T1-weighted MR image with fat saturation shows mainly cystic multiseptate mass in right and posterior neck with central enhancing soft-tissue component (*asterisk*).

often presenting with nonspecific symptoms of swelling or tenderness, features that can cause a delay in diagnosis and can cause confusion with benign processes such as lymphatic malformations [65, 66, 68]. Notably, the average duration of symptoms of SSs before diagnosis is reported to be 2–4 years [67]. On imaging, SSs can be markedly homogeneous and hyperintense on fluid-sensitive sequences, or they may be cystic because of hemorrhage or necrosis, thus mimicking lymphatic malformations [67, 69]. Cystic SSs are usually well-defined multilocular septate masses that displace rather than invade adjacent structures and that may contain fluid-fluid levels similar to those seen with lymphatic malformations [65, 70–72] (Fig. 6).

Clues to the diagnosis of SSs on imaging include the presence of a rapidly enhancing soft-tissue component, thick (> 3 mm) or nodular septa, and the triple sign on MRI [66, 67] (Fig. 6). The triple sign refers to the marked heterogeneity of the mainly cystic neoplasm with predominant areas of high signal on T2-weighted MR images but also with intermixed areas of intermediate and low signal caused by hemorrhage, necrosis, and fibrous and solid tumoral components [67, 73]. Lymphatic malformations with locules at different stages of bleeding may have a similar appearance (Fig. 1). Tumoral calcification, reported in as many as 30% of SSs, is a differentiating feature from lymphatic malformations [68, 74]. Supporting features for SSs are slow growth, notably not proportional to the patient's growth, appearance in late childhood or adolescence, and a deeply seated mass.

Angiomatoid Fibrous Histiocytoma

Angiomatoid fibrous histiocytoma is a slow-growing neoplasm of low-grade malignancy [75, 76]. Angiomatoid fibrous histiocytomas are most commonly found in the extremities of adolescents and young adults, with most occurrences outside the extremities reported in the head and neck, similar locations to those of lymphatic malformations [76, 77]. Clinically, angiomatoid fibrous histiocytomas can appear similar to lymphatic malformations, because they are also painless soft slow-growing masses [75, 78, 79]. In addition, angiomatoid fibrous histiocyto-

mas tend to have a bluish hue, with reports of rapid growth due to hemorrhage [76]. A subset of pediatric patients with angiomatoid fibrous histiocytomas present with systemic symptoms, such as malaise, weight loss, and anemia [79].

At imaging, angiomatoid fibrous histiocytomas can resemble lymphatic malformations. They are uniformly well-defined, noninvasive, and usually restricted to the subcutaneous tissues [65, 80] (Fig. 7). A literature review found few reports of MRI of angiomatoid fibrous histiocytomas, all of which reported well-circumscribed heterogeneous masses, internal cystic spaces with fluid-fluid levels, solid components being isointense to muscle on T1-weighted MR images, and marginal hypointense signal of the pseudocapsule on T1- and T2-weighted MR images [65, 78–81] (Fig. 7). The imaging appearance of angiomatoid fibrous histiocytomas has been reported as a well-demarcated multicystic subcutaneous mass having peripheral (but no internal) vascularity on Doppler examination [82], similar to one of our cases (Fig. 7).

Differentiating features on imaging include the presence of a solid enhancing component and the presence of a hypointense pseudocapsule in a multilocular cystic lesion in the case of an angiomatoid fibrous histiocytoma. The late appearance during adolescence and the presence of systemic symptoms should raise the suspicion of angiomatoid fibrous histiocytomas and prompt excisional biopsy, which is curative.

Epithelioid Sarcoma

Epithelioid sarcoma is a rare aggressive soft-tissue tumor of adolescents and young adults that most commonly occurs in the distal extremities, with a predilection for the hand [65, 83, 84]. Epithelioid sarcoma shows an indolent growth pattern and may present clinically as a heterogeneous intramuscular mass, as is characteristic of soft-tissue neoplasms [85]. However, a significant number of reports describe presentation of painless subcutaneous nodules or plaques, occasionally with overlying skin ulcerations [85].

MRI findings of epithelioid sarcoma are limited to case reports, except for two case series by Hanna et al. [86] and Romero et al. [87], showing heterogeneous soft-tissue foci and cystic areas with fluid-fluid levels reflecting necrosis (Fig. 8). Similar to lymphatic malformations, which tend to insinuate along fascial planes, epithelioid sarcoma tends to spread along the fascial planes and tendon sheaths [65, 83, 86]. The presence of peritumoral inflammation of the surrounding musculature, with a hyperintense signal on fluid-sensitive sequences, is characteristic of epithelioid sarcoma, simulating an inflamed lymphatic malformation [86, 88] (Fig. 8). Epithelioid sarcoma ubiquitously shows enhancement of the soft-tissue component, which is its main differentiating feature from lymphatic malformations [86, 88].

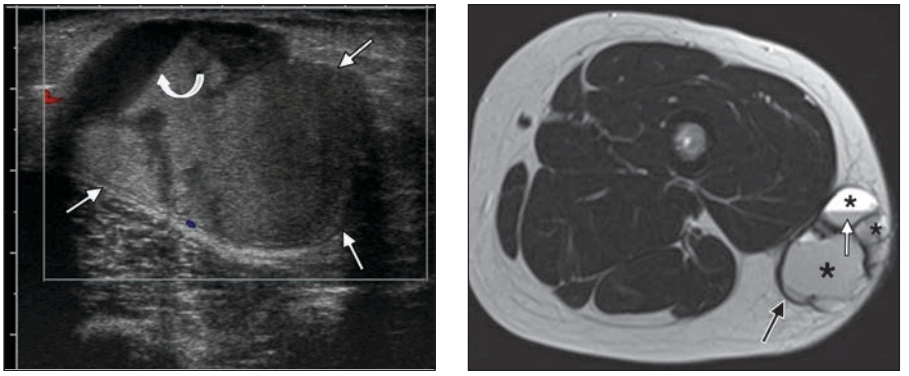

Fig. 7—14-year-old girl with angiomatoid fibrohistiocytoma presenting as slow-growing painless lump in thigh for several months with bluish discoloration.
A, High-resolution color Doppler image of thigh lesion shows lobulated well-defined mass (*straight arrows*) confined to superficial soft tissues containing low-level echoes and fluid-fluid level (*curved arrow*). No color flow is present within lesion.
B, Axial T2-weighted MR image of thigh shows lobulated well-defined mass containing locules of different intensities (*asterisks*) and fluid-fluid level (*white arrow*). Hypointense peripheral rim sign described in these lesions is well identified (*black arrow*).

Nonneoplastic Cystic Lesions That Can Mimic Lymphatic Malformations

Different types of cysts in children that involve the skin and superficial subcutaneous soft tissues can potentially mimic lymphatic malformations clinically and on imaging. Nonneoplastic cystic lesions occurring in the subcutaneous tissues include a variety of ciliated cysts, epidermoid and dermoid cysts, and ganglion cysts. These cystic lesions may share overlapping features with lymphatic malformations, including congenital cause, location (e.g., branchial cleft cysts in the head and neck or ganglion cysts in the extremities), and symptoms (e.g., lack of pain and slow growth). These cystic lesions, like lymphatic malformations, can show sudden growth with debris-filled appearance in the setting of superimposed infection, as commonly seen in dermoid and branchial cleft cysts. Epidermoid, dermoid, and ciliated cysts, which can occur anywhere in the body and often present in unexpected and unusual locations, are discussed in the next section, with comparison and contrast to features of lymphatic malformations.

Epidermoid and Dermoid Cysts

Epidermoid and dermoid cysts are the most common cutaneous cysts in both children and adults [89]. Epidermoid cysts (including sebaceous cysts) are benign lesions characterized by an ectodermal lining that undergoes desquamation producing keratin debris and, in turn, filling the cavity of the cyst [22, 90]. Dermoid cysts are similar to epidermoid cysts but also contain dermal adnexal structures, such as hair follicles or glandular tissue [91, 92]. Epidermoid and dermoid cysts are typically located in the soft tissues of the head and neck or the trunk and less frequently in the extremities [93]. Clinically, these lesions are asymptomatic at the initial stages, when they are small. A painless mobile rubbery subcutaneous nodule is a common clinical presentation [91, 94].

At US, which is the first-line imaging modality to evaluate epidermoid and dermoid cysts, these lesions are well-defined, ovoid, and cystic and exhibit posterior acoustic enhancement with heterogeneous internal appearance, likely secondary to internal keratin debris [93]. No associated vascularity is present. Occasionally, epidermoid and dermoid cysts cause osseous remodeling, resulting in thinning, scalloping, or erosion of adjacent bone. At MRI, most epidermoid cysts show mixed signals, often superimposed on a background of high signal intensity, on both T1- and T2-weighted MR images

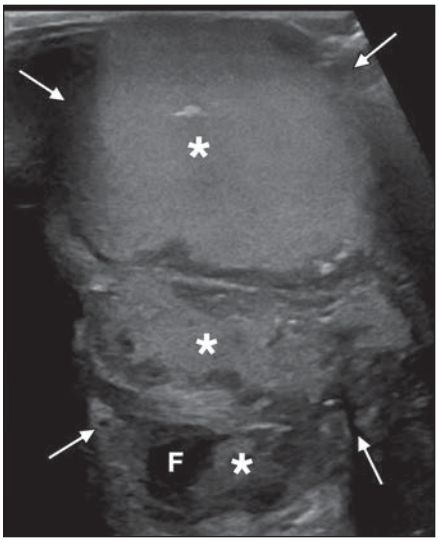

A

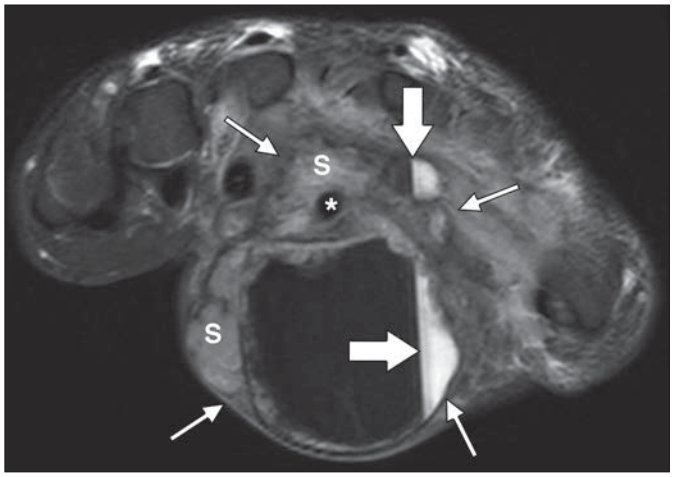

B

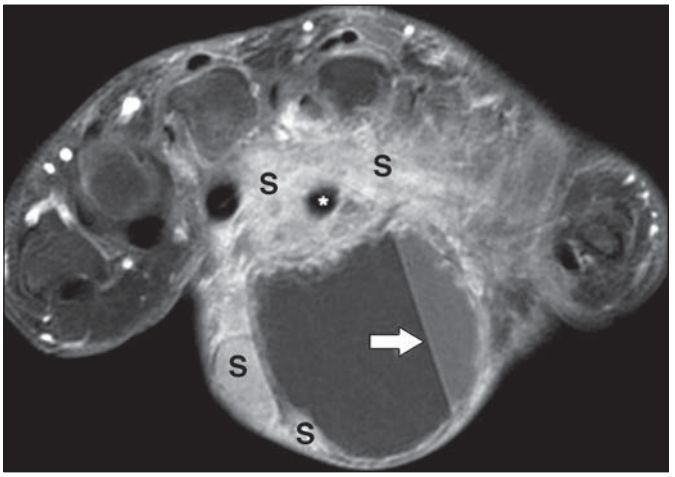

C

Fig. 8—9-year-old boy with epithelioid sarcoma presenting as acute swelling of slow-growing lump in hand.
A, High-resolution ultrasound image of hand mass shows multiseptate mass (*arrows*) with deep extension. Locules contain fluid (F) and low-level echoes (*asterisks*), likely hemorrhage.
B, Axial T2-weighted MR image with fat saturation shows predominantly cystic mass (*thin arrows*) with soft-tissue component (S) in periphery and encasing flexor tendon (*asterisk*). Fluid-fluid levels are seen (*thick arrows*); hypointense fluid within locules indicates acute hemorrhage. Significant perilesional edema is present.
C, Axial contrast-enhanced T1-weighted MR image with fat saturation shows mass with enhancement of soft-tissue component (S) in periphery and encasing flexor tendon (*asterisk*). Fluid-fluid level (*arrow*) is seen within cystic locule, as well as significant perilesional edema.

(Fig. 9), with internal heterogeneity thought to correlate histologically to keratin debris [95]. Dermoid cysts have an MRI appearance nearly identical to that of epidermoid cysts. However, they show signal dropout on fat saturation sequences, which is highly specific for dermoid cysts and also a differentiating feature from lymphatic malformations, which do not contain fat [94, 96]. These lesions have a thicker capsule than lymphatic malformations do, and they may also display faint peripheral capsular enhancement. However, septations are the exception rather than the rule, contrary to the case of lymphatic malformations, which are almost always multiloculated (Fig. 9). In infected cysts or in cases of rupture, capsular enhancement and perilesional inflammation are present. Most of these cysts pose no diagnostic difficulties clinically or by imaging. However, these lesions are congenital, can grow slowly and attain large sizes, and are painless but become infected and oc-

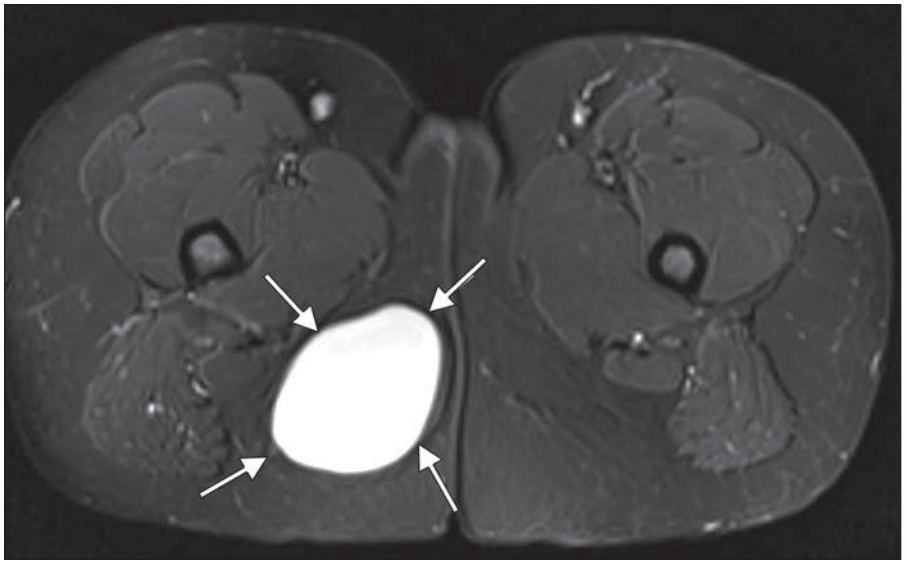

Fig. 9—15-year-old girl with dermoid cyst presenting as slow-growing painless lump in right gluteal region. Axial T2-weighted MR image with fat saturation shows large homogeneously hyperintense oval lesion (*arrows*) suggesting cystic nature. Note lack of septations.

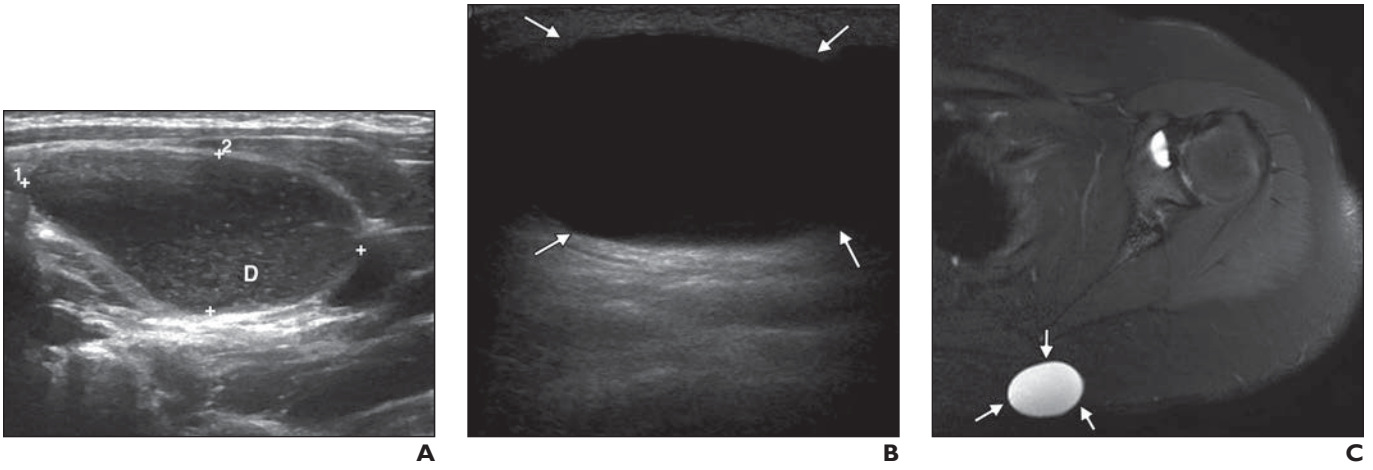

Fig. 10—Two patients with painless lumps in back and neck.
A, 7-year-old girl with branchial cleft cyst who noticed sudden development of painless rubbery lump in posterior neck. High-resolution ultrasound (US) image shows unilocular hypoechoic well-defined oval mass (inside *calipers*) with increased through-transmission containing debris (D) on dependent portion.
B and **C,** 14-year-old boy with painless lump in back for several months. High-resolution US image of back (**B**) shows well-defined oval lesion (*arrows*) with increased through-transmission containing anechoic fluid but no septations confined to superficial subcutaneous soft tissues. Axial T2-weighted MR image of shoulder (**C**) shows well-defined oval mass (*arrows*) as hyperintense confirming cystic nature. Lesion is confined to superficial subcutaneous soft tissues. No septations are present. Histologic diagnosis was cutaneous ciliated cyst, despite unusual location and male sex.

casionally septate, all features shared with lymphatic malformations.

Ciliated Cysts

Ciliated cysts are commonly classified by location: bronchogenic, thymic, enteric, thyroglossal, branchial, or cutaneous, with atypical locations reported for all types [91, 92, 97–99] (Fig. 10). Thyroglossal duct cysts and branchial cleft remnants are the two most common congenital neck masses in children, with thyroglossal duct cysts located in a midline location from the base of the tongue to the mediastinum and branchial cleft remnants (e.g., cysts and sinuses) in the lateral aspect of the neck [99, 100]. When they are in the typical locations, because of their unilocular appearance on imaging, the diagnosis is straightforward. When they are in atypical locations, such as the posterior triangle where lymphatic malformations are more common, the diagnosis is more challenging [101] (Fig. 10). Other shared features with lymphatic malformations are congenital cause, slow growth, a diagnosis in the first few years of life, and risk of infection or bleeding.

Cutaneous ciliated cysts are rare benign cysts of the superficial subcutaneous tissues and are defined by a simple columnar ciliated epithelial lining of müllerian origin [97, 102, 103]. Cutaneous ciliated cysts are classically associated as being located in the lower extremities of female patients of childbearing age, though reports exist of cutaneous ciliated cysts in various locations and in both sexes [102, 104]. Clinically, unless they are infected, these lesions present as painless subcutaneous masses, with patients seeking evaluation or excision for cosmetic reasons [97, 101, 104].

Cutaneous ciliated cysts share similar imaging characteristics with lymphatic malformations, including fluid-filled cystic spaces with no internal flow, soft-tissue component, or surrounding inflammatory changes. Neither lesion enhances on contrast agent administration, though capsular and septal enhancement and adjacent soft-tissue inflammation may be seen in acute infection, hemorrhage, or rupture (Fig. 10). Definitive imaging diagnosis may be difficult, and clinical history may not be discerning, because both ciliated cysts and lymphatic malformations are congenital. The presence of a unilocular cystic lesion in the superficial subcutaneous soft tissues should raise the possibility of a ciliated cyst rather than a lymphatic malformation. In the case of a branchial cleft cyst, the specific location in the neck is a suggestive clue. In the case of a cutaneous ciliated cyst, the patient's being a female adolescent and a lower extremity location support the diagnosis.

Conclusion

Clinical history and physical examination play vital roles in the diagnosis of pediatric subcutaneous lesions, particularly when a vascular malformation is suspected. In most cases, the diagnosis of lymphatic malformations poses no difficulty; however, the clinical and radiographic appearance can change in cases of trauma, hemorrhage, or infection. In contrast, some soft-tissue lesions, including malignant neoplasms, especially when cystic, can mimic lymphatic malformations. Therefore, the radiologist plays an important role in the diagnosis of lymphatic malformations requiring familiarity with the varied (clinical and imaging) appearance of lymphatic malformations in their undisturbed and stimulated state as well as of some pediatric soft-tissue pathologic abnormalities to avoid a delay in the diagnosis. The appearance of lymphatic malformations on imaging is fairly typical in most cases; however, a proper history and physical examination by the radiologist and preferably by an interventional radiologist in the setting of a vascular malformation clinic should be ideal, especially in equivocal cases or if image-guided intervention is contemplated. If the clinical and imaging diagnosis is still uncertain, histologic confirmation should be performed.

References

1. Fishman SJ, Mulliken JB. Hemangiomas and vascular malformations of infancy and childhood. *Pediatr Clin North Am* 1993; 40:1177–1200
2. Brouillard P, Vikkula M. Vascular malformations: localized defects in vascular morphogenesis. *Clin Genet* 2003; 63:340–351
3. Donnelly LF, Adams DM, Bisset GS. Vascular malformations and hemangiomas: a practical approach in a multidisciplinary clinic. *AJR* 2000;

174:597–608

4. Mulliken JB, Glowacki J. Hemangiomas and vascular malformations in infants and children: a classification based on endothelial characteristics. *Plast Reconstr Surg* 1982; 69:412–422
5. Fordham LA, Chung CJ, Donnelly LF. Imaging of congenital vascular and lymphatic anomalies of the head and neck. *Neuroimaging Clin N Am* 2000; 10:117–136
6. Burrows PE, Laor T, Paltiel H, et al. Diagnostic imaging in the evaluation of vascular birthmarks. *Dermatol Clin* 1998; 16:455–488
7. Brown RL, Azizkhan RG. Pediatric head and neck lesions. *Pediatr Clin North Am* 1998; 45:889–905
8. Stringel G. Hemangiomas and lymphangiomas. In: Ashcraft KW, Holder TM, eds. *Pediatric surgery*. Philadelphia, PA: Saunders, 1993:802–822
9. Brouillard P, Vikkula M. Genetic causes of vascular malformations. *Hum Mol Genet* 2007; 16(spec no 2):R140–R149
10. Love Z, Hsu DP. Low-flow vascular malformations of the head and neck: clinicopathology and image guided therapy. *J Neurointerv Surg* 2012; 4:414–425
11. Paltiel HJ, Burrows PE, Kozakewich HP, et al. Soft-tissue vascular anomalies: utility of US for diagnosis. *Radiology* 2000; 214:747–754
12. Wong KT, Lee YY, King AD, Ahuja AT. Imaging of cystic or cyst-like neck masses. *Clin Radiol* 2008; 63:613–622
13. Lee BB, Kim YW, Seo JM, et al. Current concepts in lymphatic malformation. *Vasc Endovascular Surg* 2005; 39:67–81
14. Belov S. Anatomopathological classification of congenital vascular defects. *Semin Vasc Surg* 1993; 6:219–224
15. Leu HJ. Pathoanatomy of congenital vascular malformations. In: Belov S, Loose DA, Weber J, eds. *Vascular malformations*. Reinbek, Germany: Einhorn-Presse Verlag, 1989:37–46
16. Lee BB. Changing concept on vascular malformation: no longer enigma. *Ann Vasc Dis* 2008; 1:11–19
17. International Society for the Study of Vascular Anomalies (ISSVA). ISSVA classification of vascular anomalies. ISSVA website. issva.clubexpress.com/docs.ashx?id=178348. Published April 2014. Accessed March 4, 2016
18. Puig S, Casati B, Staudenherz A, et al. Vascular low-flow malformations in children: current concepts for classification, diagnosis and therapy. *Eur J Radiol* 2005; 53:35–45
19. Restrepo R. Multimodality imaging of vascular anomalies. *Pediatr Radiol* 2013; 43(suppl 1):S141–S154
20. Willard KJ, Cappel MA, Kozin SH, et al. Congenital and infantile skin lesions affecting the hand and upper extremity. Part 1. Vascular neoplasms and malformations. *J Hand Surg Am* 2013; 38:2271–2283
21. Elluru RG, Balakrishnan K, Padua HM. Lymphatic malformations: diagnosis and management. *Semin Pediatr Surg* 2014; 23:178–185
22. Morrow MS, Oliveira AM. Imaging of lumps and bumps in pediatric patients: an algorithm for appropriate imaging and pictorial review. *Semin Ultrasound CT MR* 2014; 35:415–429
23. Flors L, Leiva-Salinas C, Maged IM, et al. MR imaging of soft-tissue vascular malformations: diagnosis, classification, and therapy follow-up. *RadioGraphics* 2011; 31:1321–1340
24. Stavros T, Rapp CL, Parker SH. Nonmalignant breast disorders that have complex cystic phases. In: Stavros T, Rapp CL, Parker SH, eds. *Breast ultrasound*, 1st ed. Philadelphia, PA: Lippincott Williams & Wilkins, 2004:351–444
25. Mirza B, Ijaz L, Saleem M, et al. Cystic hygroma: an overview. *J Cutan Aesthet Surg* 2010; 3:139–144
26. Hogeling M, Adams S, Law J, et al. Lymphatic malformations: clinical course and management in 64 cases. *Australas J Dermatol* 2011; 52:186–190
27. Jucá NBH, Crisóstomo MGR, de Oliveira LMP, et al. Acral microcystic lymphangioma: differential diagnosis in verrucous lesions of the extremities. *An Bras Dermatol* 2011; 86:343–346
28. Wang S, Krulig E, Hernandez C. Acquired microcystic lymphatic malformation of the distal upper extremity mimicking verrucae vulgaris. *Pediatr Dermatol* 2013; 30:e78–e82
29. Dubois J, Alison M. Vascular anomalies: what a radiologist needs to know. *Pediatr Radiol* 2010; 40:895–905
30. Chiou HJ, Chou YH, Chiu SY, et al. Differentiation of benign and malignant superficial soft-tissue masses using grayscale and color Doppler ultrasonography. *J Chin Med Assoc* 2009; 72:307–315
31. Griffith JF, Chan DP, Kumta SM, Chow LT, Ahuja AT. Does Doppler analysis of musculoskeletal soft-tissue tumours help predict tumour malignancy? *Clin Radiol* 2004; 59:369–375
32. Belli P, Costantini M, Mirk P, Maresca G, Priolo F, Marano P. Role of color Doppler sonography in the assessment of musculoskeletal soft tissue masses. *J Ultrasound Med* 2000; 19:823–830
33. Lee MH, Kim NR, Ryu JA. Cyst-like solid tumors of the musculoskeletal system: an analysis of ultrasound findings. *Skeletal Radiol* 2010; 39:981–986
34. Thacker MM. Malignant soft tissue tumors in children. *Orthop Clin North Am* 2013; 44:657–667
35. Tsai JC, Dalinka MK, Fallon MD, et al. Fluid-fluid level: a nonspecific finding in tumors of bone and soft tissue. *Radiology* 1990; 175:779–782
36. Alyas F, Lee J, Ahmed M, et al. Prevalence and diagnostic significance of fluid-fluid levels in soft-tissue neoplasms. *Clin Radiol* 2007; 62:769–774
37. Keenan S, Bui-Mansfield LT. Musculoskeletal lesions with fluid-fluid level: a pictorial essay. *J Comput Assist Tomogr* 2006; 30:517–524
38. Van Dyck P, Vanhoenacker FM, Vogel J, et al. Prevalence, extension and characteristics of fluid-fluid levels in bone and soft tissue tumors. *Eur Radiol* 2006; 16:2644–2651
39. Isaacs H. Congenital and neonatal malignant tumors: a 28-year experience at Children's Hospital of Los Angeles. *Am J Pediatr Hematol Oncol* 1987; 9:121–129
40. Stevens MC. Neonatal tumours. *Arch Dis Child* 1988; 63(spec no 10):1122–1125
41. Moore SW. Neonatal tumours. *Pediatr Surg Int* 2013; 29:1217–1229
42. Parkes SE, Muir KR, Southern L, et al. Neonatal tumours: a thirty-year population-based study. *Med Pediatr Oncol* 1994; 22:309–317
43. Birch JM, Blair V. The epidemiology of infant cancers. *Br J Cancer Suppl* 1992; 18:S2–S4
44. McCarville MB, Kaste SC, Pappo AS. Soft-tissue malignancies in infancy. *AJR* 1999; 173:973–977
45. Isaacs H. Perinatal (congenital and neonatal) neoplasms: a report of 110 cases. *Pediatr Pathol* 1985; 3:165–216
46. Smirniotopoulos JG, Chiechi MV. Teratomas, dermoids, and epidermoids of the head and neck. *RadioGraphics* 1995; 15:1437–1455
47. Barksdale EM, Obokhare I. Teratomas in infants and children. *Curr Opin Pediatr* 2009; 21:344–349
48. Woodward PJ, Sohaey R, Kennedy A, et al. From the archives of the AFIP: a comprehensive review of fetal tumors with pathologic correlation. *RadioGraphics* 2005; 25:215–242
49. Garmel SH, Crombleholme TM, Semple JP, et al. Prenatal diagnosis and management of fetal tumors. *Semin Perinatol* 1994; 18:350–365
50. Moeller KH, Rosado-de-Christenson ML, Templeton PA. Mediastinal mature teratoma: imaging features. *AJR* 1997; 169:985–990
51. Bhutta MF, Ching H-Y, Hartley BE. Cervico-thoracic teratoma masquerading as lymphatic malformation. *J Laryngol Otol* 2006; 120:955–958
52. Andronikou S, Kumbla S, Fink AM. Neonatal nasopharyngeal teratomas: cross sectional imaging findings. *Pediatr Radiol* 2003; 33:241–246
53. April MM, Ward RF, Garelick JM. Diagnosis, management, and follow-up of congenital head and neck teratomas. *Laryngoscope* 1998; 108:1398–1401
54. Carr MM, Thorner P, Phillips JH. Congenital teratomas of the head and neck. *J Otolaryngol* 1997; 26:246–252
55. Zielinski R, Respondek-Liberska M. Retrospective chart review of 44 fetuses with cervicofacial tumors in the sonographic assessment. *Int J Pediatr Otorhinolaryngol* 2015; 79:363–368
56. Megarbane H, Doz F, Manach Y, et al. Neonatal rhabdomyosarcoma misdiagnosed as a congenital

hemangioma. *Pediatr Dermatol* 2011; 28:299–301
57. Robson CD. Imaging of head and neck neoplasms in children. *Pediatr Radiol* 2010; 40:499–509
58. Rosen A, Jedynak AR, Respler D. Lipoblastoma of the neck mimicking cystic hygroma. *Otolaryngol Head Neck Surg* 2005; 132:511–513
59. Chen C-W, Chang W-C, Lee H-S, et al. MRI features of lipoblastoma: differentiating from other palpable lipomatous tumor in pediatric patients. *Clin Imaging* 2010; 34:453–457
60. Bruyeer E, Lemmerling M, Poorten VV, et al. Paediatric lipoblastoma in the head and neck: three cases and review of literature. *Cancer Imaging* 2012; 12:484–487
61. Reiseter T, Nordshus T, Borthne A, et al. Lipoblastoma: MRI appearances of a rare paediatric soft tissue tumour. *Pediatr Radiol* 1999; 29:542–545
62. Harrer J, Hammon G, Wagner T, et al. Lipoblastoma and lipoblastomatosis: a report of two cases and review of the literature. *Eur J Pediatr Surg* 2001; 11:342–349
63. Pham NS, Poirier B, Fuller SC, et al. Pediatric lipoblastoma in the head and neck: a systematic review of 48 reported cases. *Int J Pediatr Otorhinolaryngol* 2010; 74:723–728
64. Moholkar S, Sebire NJ, Roebuck DJ. Radiological-pathological correlation in lipoblastoma and lipoblastomatosis. *Pediatr Radiol* 2006; 36:851–856
65. Laffan EE, Ngan B-Y, Navarro OM. Pediatric soft-tissue tumors and pseudotumors: MR imaging features with pathologic correlation. Part 2. Tumors of fibroblastic/myofibroblastic, so-called fibrohistiocytic, muscular, lymphomatous, neurogenic, hair matrix, and uncertain origin. *RadioGraphics* 2009; 29:e36
66. Bakri A, Shinagare AB, Krajewski KM, et al. Synovial sarcoma: imaging features of common and uncommon primary sites, metastatic patterns, and treatment response. *AJR* 2012; 199:[web]W208–W215
67. Murphey MD, Gibson MS, Jennings BT, et al. From the archives of the AFIP: imaging of synovial sarcoma with radiologic-pathologic correlation. *RadioGraphics* 2006; 26:1543–1565
68. Bixby SD, Hettmer S, Taylor GA, et al. Synovial sarcoma in children: imaging features and common benign mimics. *AJR* 2010; 195:1026–1032
69. Marzano L, Failoni S, Gallazzi M, et al. The role of diagnostic imaging in synovial sarcoma: our experience. *Radiol Med (Torino)* 2004; 107:533–540
70. Tateishi U, Hasegawa T, Beppu Y, et al. Synovial sarcoma of the soft tissues: prognostic significance of imaging features. *J Comput Assist Tomogr* 2004; 28:140–148
71. Blacksin MF, Siegel JR, Benevenia J, et al. Synovial sarcoma: frequency of nonaggressive MR characteristics. *J Comput Assist Tomogr* 1997; 21:785–789
72. Nakanishi H, Araki N, Sawai Y, et al. Cystic synovial sarcomas: imaging features with clinical and histopathologic correlation. *Skeletal Radiol* 2003; 32:701–707
73. Jones BC, Sundaram M, Kransdorf MJ. Synovial sarcoma: MR imaging findings in 34 patients. *AJR* 1993; 161:827–830
74. Eilber FC, Dry SM. Diagnosis and management of synovial sarcoma. *J Surg Oncol* 2008; 97:314–320
75. Daw NC, Billups CA, Pappo AS, et al. Malignant fibrous histiocytoma and other fibrohistiocytic tumors in pediatric patients: the St. Jude Children's Research Hospital experience. *Cancer* 2003; 97:2839–2847
76. Bohman SL, Goldblum JR, Rubin BP, et al. Angiomatoid fibrous histiocytoma: an expansion of the clinical and histological spectrum. *Pathology* 2014; 46:199–204
77. Enzinger FM. Angiomatoid malignant fibrous histiocytoma: a distinct fibrohistiocytic tumor of children and young adults simulating a vascular neoplasm. *Cancer* 1979; 44:2147–2157
78. Ajlan AM, Sayegh K, Powell T, et al. Angiomatoid fibrous histiocytoma: magnetic resonance imaging appearance in 2 cases. *J Comput Assist Tomogr* 2010; 34:791–794
79. Li CS, Chan WP, Chen WT, et al. MRI of angiomatoid fibrous histiocytoma. *Skeletal Radiol* 2004; 33:604–608
80. Murphey MD, Gross TM, Rosenthal HG. From the archives of the AFIP: musculoskeletal malignant fibrous histiocytoma—radiologic-pathologic correlation. *RadioGraphics* 1994; 14:807–826
81. Bauer A, Jackson B, Marner E, et al. Angiomatoid fibrous histiocytoma: a case report and review of the literature. *J Radiol Case Rep* 2012; 6:8–15
82. Hata H, Natsuga K, Aoyagi S, et al. Ultrasound B-mode and elastographic findings of angiomatoid fibrous histiocytoma. *Clin Exp Dermatol* 2014; 39:538–539
83. Casanova M, Ferrari A, Collini P, et al. Epithelioid sarcoma in children and adolescents: a report from the Italian Soft Tissue Sarcoma Committee. *Cancer* 2006; 106:708–717
84. Beaman FD, Kransdorf MJ, Andrews TR, et al. Superficial soft-tissue masses: analysis, diagnosis, and differential considerations. *RadioGraphics* 2007; 27:509–523
85. Wolf PS, Flum DR, Tanas MR, et al. Epithelioid sarcoma: the University of Washington experience. *Am J Surg* 2008; 196:407–412
86. Hanna SL, Kaste S, Jenkins JJ, et al. Epithelioid sarcoma: clinical, MR imaging and pathologic findings. *Skeletal Radiol* 2002; 31:400–412
87. Romero JA, Kim EE, Moral IS. MR characteristics of epithelioid sarcoma. *J Comput Assist Tomogr* 1994; 18:929–931
88. Tateishi U, Hasegawa T, Kusumoto M, et al. Radiologic manifestations of proximal-type epithelioid sarcoma of the soft tissues. *AJR* 2002; 179:973–977
89. Golden BA, Zide MF. Cutaneous cysts of the head and neck. *J Oral Maxillofac Surg* 2005; 63:1613–1619
90. Koeller KK, Alamo L, Adair CF, et al. Congenital cystic masses of the neck: radiologic-pathologic correlation. *RadioGraphics* 1999; 19:121–146
91. Li WY, Reinisch JF. Cysts, pits, and tumors. *Plast Reconstr Surg* 2009; 124(suppl):106e–116e
92. Acierno SP, Waldhausen JHT. Congenital cervical cysts, sinuses and fistulae. *Otolaryngol Clin North Am* 2007; 40:161–176
93. Lee HS, Joo KB, Song HT, et al. Relationship between sonographic and pathologic findings in epidermal inclusion cysts. *J Clin Ultrasound* 2001; 29:374–383
94. Berry T, Shetty A, Delu A, et al. Presternal dermoid cyst mimicking lymphatic malformation: a case report and review of the literature. *Pediatr Dermatol* 2013; 30:128–130
95. Hong SH, Chung HW, Choi JY, et al. MRI findings of subcutaneous epidermal cysts: emphasis on the presence of rupture. *AJR* 2006; 186:961–966
96. Ro EY, Thomas RM, Isaacson GC. Giant dermoid cyst of the neck can mimic a cystic hygroma: using MRI to differentiate cystic neck lesions. *Int J Pediatr Otorhinolaryngol* 2007; 71:653–658
97. Fontaine DG, Lau H, Murray SK, et al. Cutaneous ciliated cyst of the abdominal wall: a case report with a review of the literature and discussion of pathogenesis. *Am J Dermatopathol* 2002; 24:63–66
98. Kurban RS, Bhawan J. Cutaneous cysts lined by nonsquamous epithelium. *Am J Dermatopathol* 1991; 13:509–517
99. Waldhausen JH. Branchial cleft and arch anomalies in children. *Semin Pediatr Surg* 2006; 15:64–69
100. LaRiviere CA, Waldhausen JH. Congenital cervical cysts, sinuses, and fistulae in pediatric surgery. *Surg Clin North Am* 2012; 92:583–597
101. Panchbhai AS, Choudhary MS. Branchial cleft cyst at an unusual location: a rare case with a brief review. *Dentomaxillofac Radiol* 2012; 41:696–702
102. Farmer ER, Helwig EB. Cutaneous ciliated cysts. *Arch Dermatol* 1978; 114:70–73
103. Rodrigo-Nicolás B, Terrádez Raro JJ, Armengot-Carbó M, et al. Müllerian and eccrine cutaneous ciliated cysts: two different entities? The contribution of WT-1 and PAX8 to diagnosis. *J Cutan Pathol* 2013; 40:608–610
104. Chong SJ, Kim SY, Kim HS, et al. Cutaneous ciliated cyst in a 16-year-old girl. *J Am Acad Dermatol* 2007; 56:159–160

FOR YOUR INFORMATION

The reader's attention is directed to part 2 accompanying this article, titled "Low-Flow Vascular Malformation Pitfalls: From Clinical Examination to Practical Imaging Evaluation—Part 2, Venous Malformation Mimickers".